

RESEARCH LETTER

10.1002/2017GL073420

Key Points:

- Rarely reported chorus emissions with long-lived (up to 25 s) oscillating tones were observed in space
- Oscillating tones can behave either regularly or irregularly and even transform into constant tones
- Oscillating tones could be nonlinearly triggered by the accompanying hiss-like band or could be related to the modulation of the wave source

Supporting Information:

- Supporting Information S1

Correspondence to:

Z. Su,
szpe@mail.ustc.edu.cn

Citation:

Gao, Z., Z. Su, L. Chen, H. Zheng, Y. Wang and S. Wang (2017), Van Allen Probes observations of whistler-mode chorus with long-lived oscillating tones, *Geophys. Res. Lett.*, *44*, 5909–5919, doi:10.1002/2017GL073420.

Received 11 MAR 2017

Accepted 1 JUN 2017

Accepted article online 6 JUN 2017

Published online 22 JUN 2017

Van Allen Probes observations of whistler-mode chorus with long-lived oscillating tones

Zhonglei Gao^{1,2,3} , Zhenpeng Su^{1,2} , Lunjin Chen⁴ , Huinan Zheng^{1,2} , Yuming Wang¹ , and Shui Wang¹

¹CAS Key Laboratory of Geospace Environment, Department of Geophysics and Planetary Sciences, University of Science and Technology of China, Hefei, China, ²Collaborative Innovation Center of Astronautical Science and Technology, University of Science and Technology of China, Hefei, China, ³Mengcheng National Geophysical Observatory, School of Earth and Space Sciences, University of Science and Technology of China, Hefei, China, ⁴Department of Physics, University of Texas at Dallas, Richardson, Texas, USA

Abstract Whistler-mode chorus plays an important role in the radiation belt electron dynamics. In the frequency-time spectrogram, chorus often appears as a hiss-like band and/or a series of short-lived (up to ~ 1 s) discrete elements. Here we present some rarely reported chorus emissions with long-lived (up to 25 s) oscillating tones observed by the Van Allen Probes in the dayside (MLT ~ 9 –14) midlatitude ($|MLAT| > 15^\circ$) region. An oscillating tone can behave either regularly or irregularly and can even transform into a nearly constant tone (with a relatively narrow frequency sweep range). We suggest that these highly coherent oscillating tones were generated naturally rather than being related to some artificial VLF transmitters. Possible scenarios for the generation of the oscillating tone chorus are as follows: (1) being nonlinearly triggered by the accompanying hiss-like bands or (2) being caused by the modulation of the wave source. The details of the generation and evolution of such a long-lived oscillating tone chorus need to be investigated both theoretically and experimentally in the future.

1. Introduction

Whistler-mode chorus is an important plasma emission controlling the Van Allen radiation belt electron behaviors [e.g., *Horne and Thorne*, 1998; *Summers et al.*, 1998, 2002; *Horne et al.*, 2005; *Reeves et al.*, 2013; *Thorne et al.*, 2013; *Su et al.*, 2014a, 2014b]. Chorus waves are believed to be excited by substorm-injected energetic electrons through the cyclotron resonance near the geomagnetic equator outside the plasmapause [e.g., *Kennel and Petschek*, 1966; *Helliwell*, 1967; *Thorne and Kennel*, 1967; *Kennel*, 1969; *Omura et al.*, 2008; *Li et al.*, 2009; *Su et al.*, 2014c]. These waves typically occur in the frequency range of 0.1 – $0.8 f_{ce}$ (with the equatorial electron gyrofrequency f_{ce}) [*Burtis and Helliwell*, 1976; *Tsurutani and Smith*, 1974; *Meredith et al.*, 2001; *Santolik et al.*, 2003a, 2004] and can arise in the low-frequency range $< 0.1 f_{ce}$ [*Cattell et al.*, 2015; *Gao et al.*, 2016] during the main phase of some geomagnetic storms.

In the frequency-time spectrogram, chorus emissions often appear as a series of discrete elements (e.g., risers, fallers, and hooks) and/or a structureless hiss-like band [*Burtis and Helliwell*, 1976; *Smith and Nunn*, 1998; *Santolik et al.*, 2004, 2009; *Li et al.*, 2012]. These discrete elements with a short duration of 0.1 – 1.0 s have been considered to be a result of the nonlinear cyclotron resonance [e.g., *Nunn et al.*, 2005; *Omura et al.*, 2008; *Omura and Nunn*, 2011; *Nunn and Omura*, 2012]. The nonlinear resonant current parallel to the wave magnetic field can cause the frequency sweep of chorus elements [*Omura and Nunn*, 2011]. The absence of the parallel resonant current would produce constant tone chorus without the frequency sweep [*Omura and Nunn*, 2011]. The hiss-like chorus band can be described as a group of dense risers nonlinearly generated at different times and locations [*Kato and Omura*, 2013].

A type of hook that appears as a combination of multiple rising and falling tones is usually referred to as the oscillating tone [*Helliwell*, 1967]. Since 1960s, many oscillating tone chorus events have been observed on the ground [e.g., *Hansen*, 1963; *Mielke et al.*, 1992; *Smith and Nunn*, 1998]. In contrast, space-based measurements of oscillating tones are very limited. Two examples of such oscillating tones have been made by the CLUSTER [*Pickett et al.*, 2005, Figure 1] and Van Allen Probes [*Hospodarsky et al.*, 2016, Figure 10.3c] missions. In the recent laboratory simulations [*Van Compernelle et al.*, 2015, Figures 3d and 3e], the oscillating tones can also be

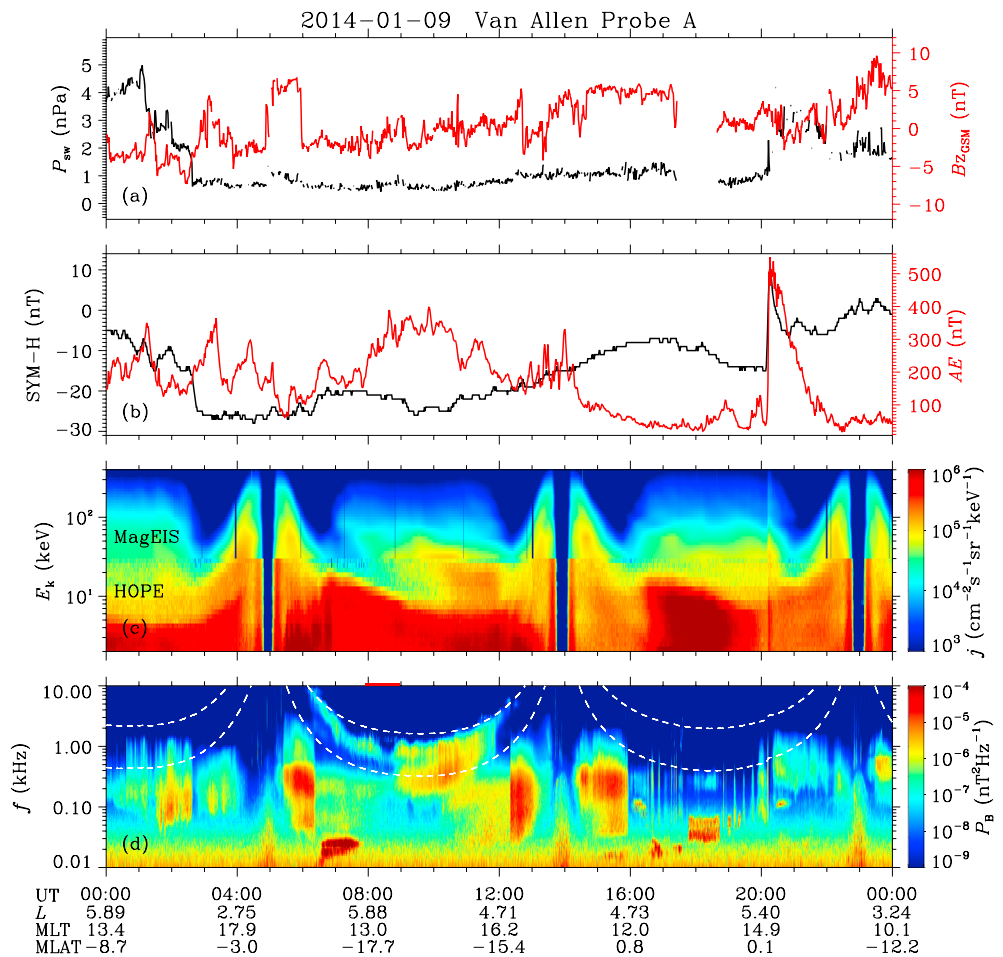


Figure 1. Overview of the space environment on 9 January 2014: (a) Solar wind dynamic pressure P_{sw} and Z component of the interplanetary magnetic field in GSM coordinate B_{zGSM} ; (b) geomagnetic activity indices AE and SYM-H; (c) electron differential flux j ; and (d) wave magnetic power spectral density P_B . The red thick line at the top of Figure 1d denotes the time range during which the oscillating tones occurred. The dashed lines in Figure 1d represent 0.1 and 0.5 f_{ce} .

identified. The typical duration of oscillating tones are found to be approximately 2–4 s [e.g., Smith and Nunn, 1998; Pickett et al., 2005], and a ground measurement of a long-lived (up to a few minutes) oscillating tone has been reported [Carpenter, 2014, Figure 5.46]. In this letter, we present some unusual chorus emissions with long-lived (up to 25 s) oscillating tones observed by the Van Allen Probes [Mauk et al., 2013] in the dayside midlatitude region.

2. Data and Method

The Van Allen Probes, which have elliptical orbits, aim to discover the fundamental physics of the Van Allen radiation belts [Mauk et al., 2013]. In this study, we mainly use data collected by the Electric and Magnetic Field Instrument Suite and Integrated Science (EMFISIS) [Kletzing et al., 2013] suite, the Electric Field and Wave (EFW) instrument [Wygant et al., 2013], and the Energetic Particle, Composition, and Thermal Plasma Suite (ECT) [Spence et al., 2013]. The background magnetic field B_0 with a 64 Hz sampling rate was observed by the tri-axial fluxgate magnetometer (MAG) of the EMFISIS suite. The corresponding equatorial magnetic field B_e can be estimated as $B_e = B_0 B_{Me} / B_{Mo}$, where B_{Me} / B_{Mo} is the ratio of equatorial magnetic field to local magnetic field in the TS04 model [Tsyganenko and Sitnov, 2005]. The cold electron density n_e with a 16 Hz sampling rate was inferred from the spacecraft potential provided by the EFW instrument. The wave power spectral density in the survey mode and the continuous-burst waveforms were provided by the Waveform Receiver of the EMFISIS Waves instrument. Each waveform block covered approximately 6 s with a 35 kHz sampling

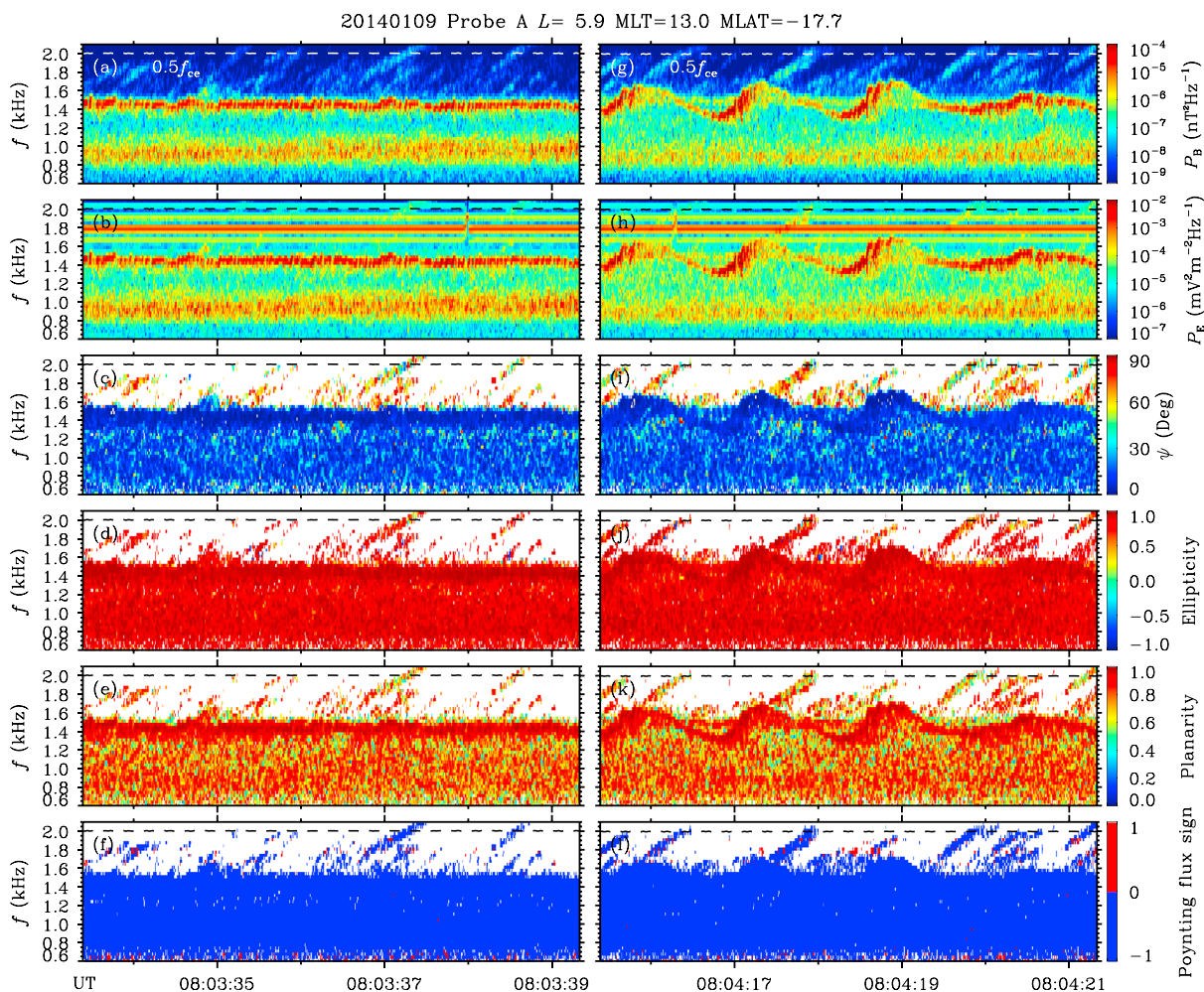


Figure 2. Unusual chorus with constant (left column) and oscillating (right column) tone around 08:04 UT on 9 January 2014. (a, b, g, and h) Magnetic and electric power spectral densities P_B and P_E (70% overlapped FFT); (c, d, e, i, j, and k) corresponding wave normal angle ψ , ellipticity, and planarity; (f and l) sign of the Poynting flux parallel to the background magnetic field (positive value for the northward direction and negative value for the southward direction).

rate. We apply a 1024 point fast Fourier transform (FFT) to these waveforms to obtain the wave spectral matrices and then use the singular value decomposition method [Santolik et al., 2003b] to determine the wave propagation characteristics. We also apply the Morlet wavelet transform to these waveforms to identify the frequency variation of chorus subpackets. The hot electrons associated with chorus wave generation were measured by the Helium, Oxygen, Proton, and Electron (HOPE) Mass Spectrometer [Funsten et al., 2013] and the Magnetic Electron Ion Spectrometer (MagEIS) [Blake et al., 2013] of the ECT suite. The space environment parameters for the events reported here were taken from the OMNI database of CDAweb [King and Papitashvili, 2005].

3. Observations

Figure 1 gives an overview of the space environment observed by Probe A on 9 January 2014. The dayside chorus waves were mainly observed in the time period 06:20–12:20 UT. In this time range of interest, there were some weak substorms ($AE < 400$ nT) but no storms ($SYM-H > -30$ nT). In response to the substorms, the electron fluxes at energies below 20 keV exhibited an obvious enhancement, favoring the generation of chorus waves. Figure 2 shows two examples of unusual chorus emissions at approximately 08:03:36 UT and 08:04:18 UT on 9 January 2014. These emissions were right-hand circularly polarized (with ellipticity values > 0.5) and propagated toward the South Pole (with Poynting fluxes antiparallel to the background magnetic field). The wave power in the frequency range of $0.1-0.5 f_{ce}$ was distributed in three parts. The upper part above the frequency 1.6 kHz consisted of a series of rising tones propagating highly oblique ($\psi > 60^\circ$) to the

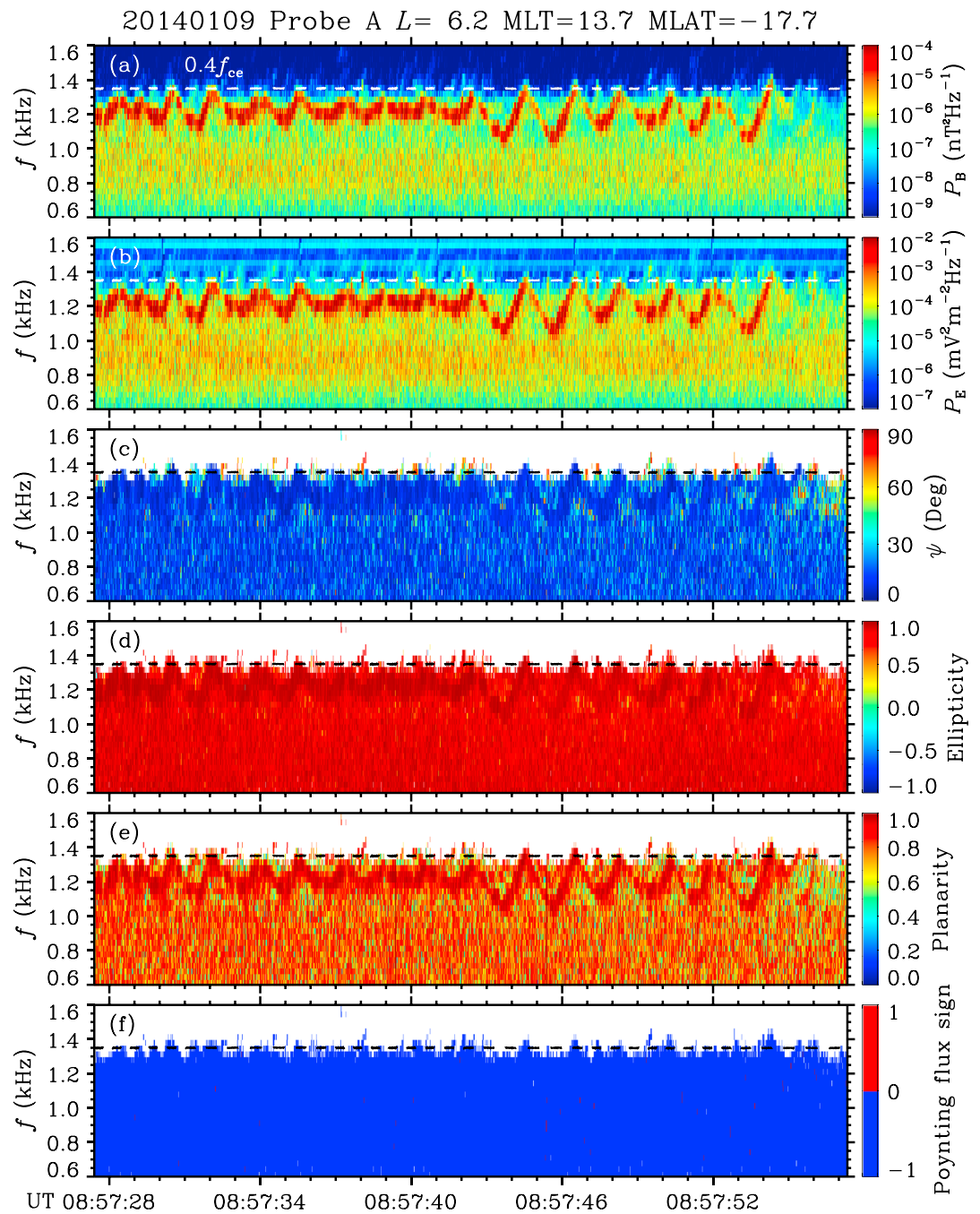


Figure 3. Similar to Figure 2, except for the time range of 08:57:28–08:57:57 UT on 9 January 2014.

background magnetic field. The lower part was a quasi-parallel ($\psi < 10^\circ$) hiss-like band in the frequency range of 0.7–1.2 kHz. The middle part appeared as a long-lived and highly coherent (with planarity values close to 1) constant or oscillating tone with quasi-parallel propagation ($\psi < 10^\circ$). The constant tone had a relatively narrow frequency range around 1.45 kHz, while the central frequency of the oscillating tone regularly swept over a range of 1.2–1.7 kHz with a repetition period of ~ 1.4 s. Over every period of the oscillating tone, the rising part with a duration of ~ 0.5 s had a larger power spectral density than that of the falling part with a duration of ~ 0.9 s. Figure 3 exhibits the transformation process between constant and oscillating tones covering 5 blocks of waveform data in the time range from 08:57:28 to 08:57:57 UT on 9 January 2014. Around 08:57:36 UT, the frequency sweep range was narrowed down to $\sim < 100$ Hz, and the oscillating tone

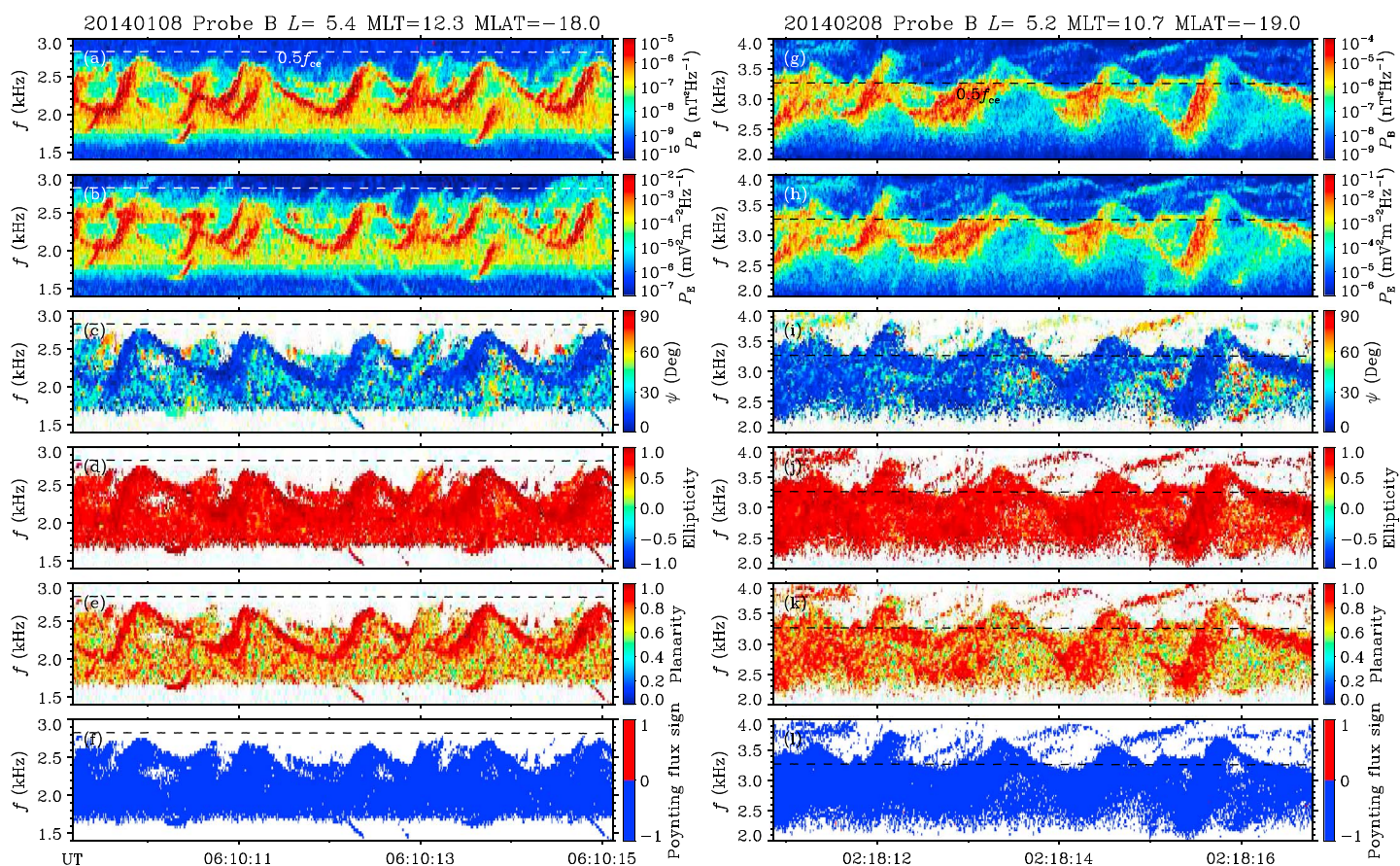


Figure 4. Similar to Figure 2, except for 8 January and 8 February 2014.

became a nearly constant tone. Approximately 6 s later, the oscillating tone with a frequency sweep range of ~400 Hz reformed. These observations suggest that the constant and oscillating tones were likely to be two manifestations of a physical process.

In fact, chorus with oscillating tones can also be found at other times. Figure 4 shows two additional events of chorus with regularly oscillating tones observed by Van Allen Probe B on 8 January 2014 and 8 February 2014. In both events, the rising parts had larger wave intensities and higher frequency sweep rates than the falling parts, consistent with the event in Figure 2. For the event on 8 January 2014, some rising tones are found to overlap with the oscillating tone. For the event on 8 February 2014, we could identify two oscillating tones in the same frequency range of 2.5–3.8 kHz. Figure 5 exhibits two examples of irregularly oscillating tones observed by Van Allen Probe B on 8 February 2014 (during the same hour as in the previous case) and 22 December 2015. In contrast to the situation of the regularly oscillating tones, the rising parts and falling parts of the irregularly oscillating tones did not show much difference with respect to the intensity and frequency sweep rate. In the event on 22 December 2015, the oscillating tone had a large wave normal angle (>60°), quite different from the other events. For these events (Figures 2–5), the oscillating tones were detected in the dayside (MLT ~9–14) midlatitude (|MLAT| > 15°) region, and the corresponding magnetosphere was experiencing some weak or moderate substorms (Figures 1 and S1–S3).

4. Discussion

4.1. Nonlinear Generation

Figure 6 plots a frequency-time spectrogram associated with the formation of a constant tone. Around 07:54:23 UT on 9 January 2014, the hiss-like band triggered a rising tone, and approximately 2 s later, the rising tone evolved into a constant tone. Figures 5a and 5g also show that these oscillating tones originated from the hiss-like bands. Figure 4a demonstrates that these rising parts of the oscillating tones had

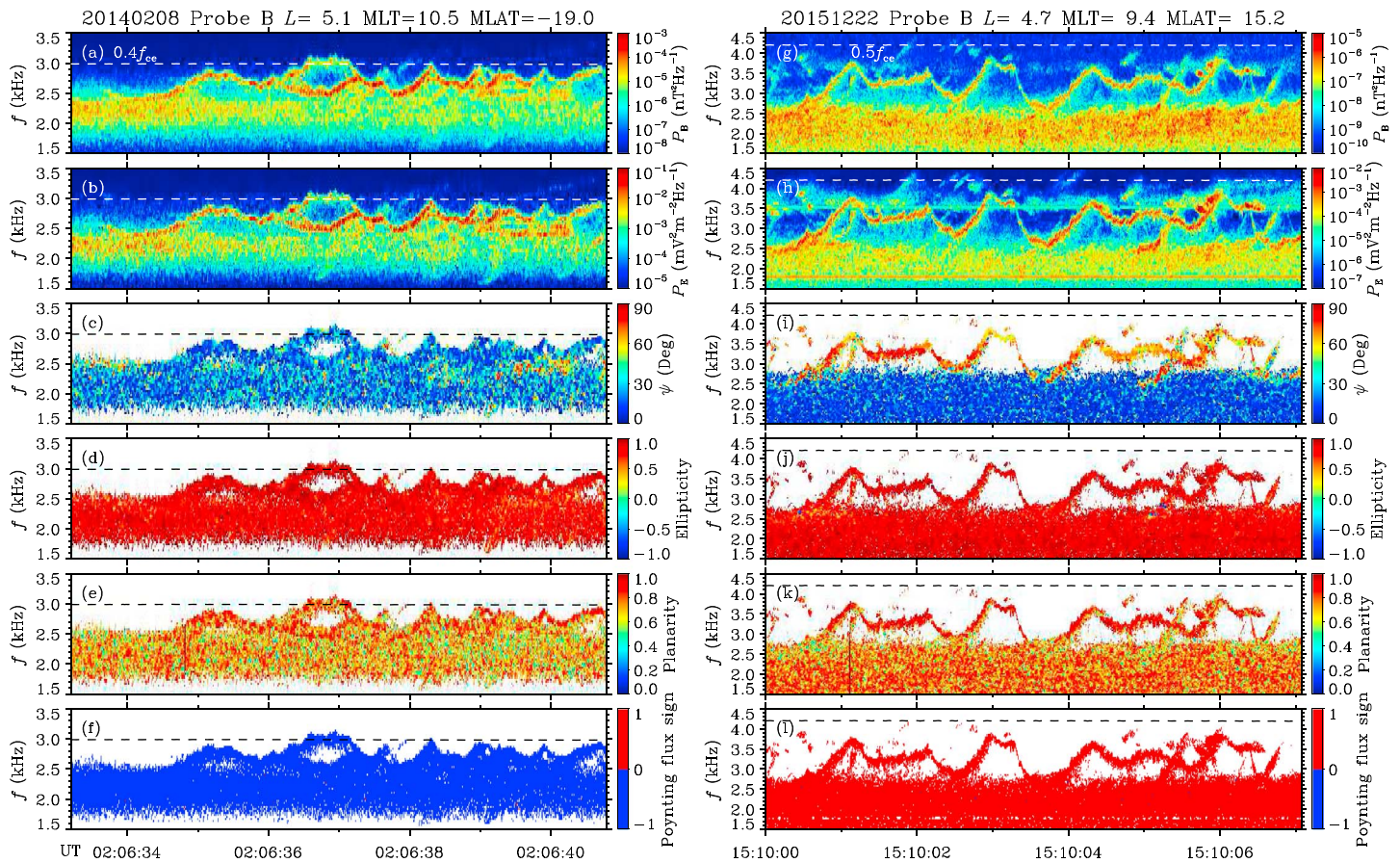


Figure 5. Similar to Figure 2, except for 8 February 2014 and 22 December 2015.

spectral shapes analogous to those of the accompanying discrete rising tones. These observations imply that the highly coherent oscillating tones might be nonlinearly triggered by the accompanying hiss-like bands [Hansen, 1963; Helliwell, 1967].

In the past, many physical mechanisms have been proposed to explain the frequency sweep of chorus elements. Hansen [1963] suggested that the wave frequency sweep was caused by the phase bunched electron motion along the field line. Helliwell [1967] introduced the term “interaction region” that can be viewed as a backward wave oscillator [Brice, 1963] and explained that the oscillating tones were a result of the drift of interaction region. Smith and Nunn [1998] suggested that the frequency sweep was caused by the nonlinear resonant current parallel to the wave magnetic field (unambiguously expressed by Nunn [1990]). The frequency sweep of chorus elements has been successfully reproduced within the framework of nonlinear cyclotron resonance [e.g., Omura et al., 2008; Omura and Nunn, 2011; Nunn and Omura, 2012]. Whether the sweep rate of a chorus element is positive or negative is determined by the location of the wave generation region [Smith and Nunn, 1998]. The riser generation region is mainly confined to the downstream of the equator, while the upstream of the equator generally tends to generate fallers [Omura and Nunn, 2011; Nunn and Omura, 2012]. Hence, a periodic transfer between these two types of generation regions [Smith and Nunn, 1998] will yield an oscillating tone. However, the nonlinear evolution of chorus could last for approximately 25 s (Figure 3), at least 1 order of magnitude larger than the duration of typical chorus elements. How a nonlinear process could self-sustain over such a long time is a mystery.

As shown in Figures 2–5, these oscillating/constant tones seemingly comprised some subpackets with much shorter durations (<0.07 s). In Figure 7, we select three segments (a constant tone and a rising and a falling part of oscillating tones) with the most obvious subpackets. For the FFT transform, we choose an overlapping rate 85% after many tests to obtain sufficiently good resolutions with respect to both frequency and time.

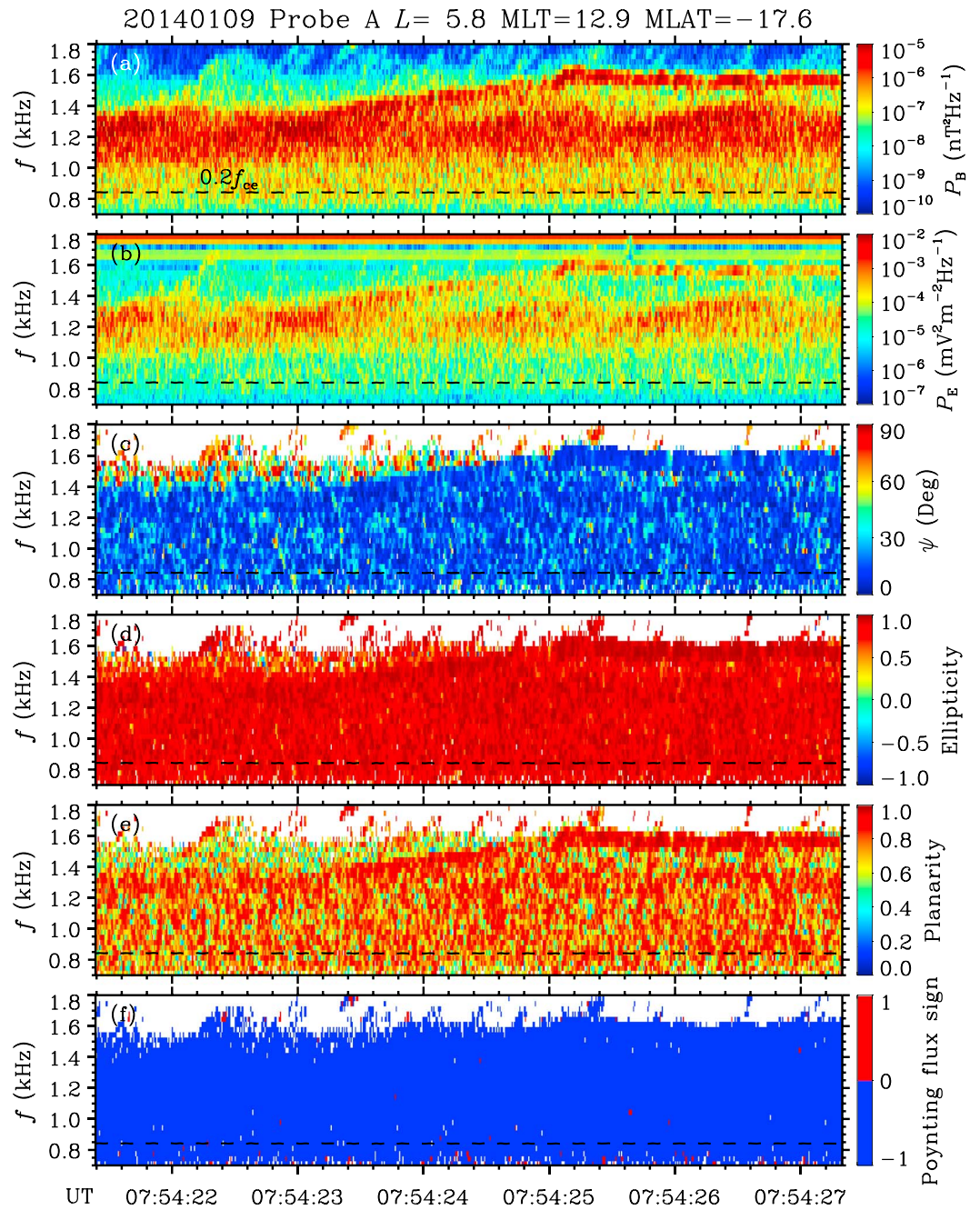


Figure 6. Similar to Figure 2, except for the time around 07:54 UT on 9 January 2014.

In addition to the regular FFT spectra, we show the FFT spectra P_{FFT}^n normalized by the maximum of chorus wave power P_{max} in a centered time window of ~ 0.06 s, and the wavelet power P_{wavelet}^n normalized by the maximum chorus wave power at each time point. One can outline the subpackets with rising frequencies for the first two segments, analogous to the situation shown by *Santolik et al.* [2014]. For the third segment, because of the small amplitudes, short durations, and narrow frequency ranges, the rising frequency feature of subpackets tended to be indistinct. In fact, for most falling parts, the frequency sweeping characteristics of the subpackets were unclear (Figures S4–S6). If the subpackets commonly have the rising frequency feature, the wave generation region will always be located downstream of the equator [Smith and Nunn, 1998] and the scenario that the transfer of generation region produces the oscillating tones will be doubtful.

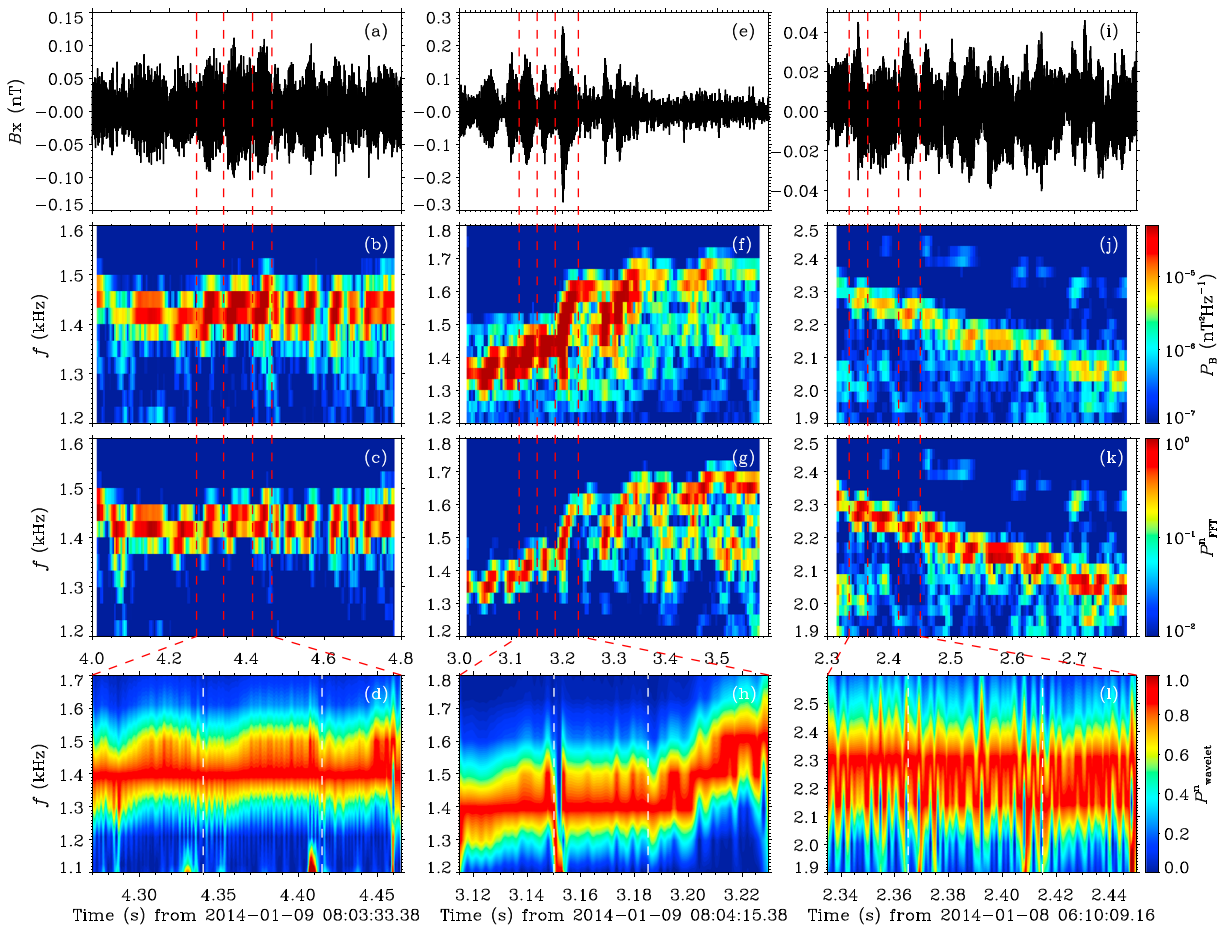


Figure 7. Detailed information regarding the segments selected from a constant tone (left column), and a rising part (middle column), and a falling part (right column) of oscillating tones: (a, e, and i) waveform of the B_x component in a local magnetic field coordinate system; (b, f, and j) magnetic power spectral density P_B (85% overlapped FFT); (c, g, and k) normalized FFT power P_{FFT}^n ; (d, h, and l) zoomed-in normalized wavelet power $P_{wavelet}^n$ of three successive subpackets of the B_x component. The vertical dashed lines are overlotted to identify the subpackets.

4.2. Modulation

The periodic variation of whistler-mode waves is usually attributed to some modulation processes [Li *et al.*, 2011a, 2011b; Colpitts *et al.*, 2016]. For these highly coherent oscillating tones, a possible generation scenario could be the combination of nonlinear generation and modulation (i.e., the wave subpackets were generated via a nonlinear process, and the starting/ending frequencies of subpackets were modulated by some physical quantities). In Figure 8, we compare the background magnetic field/density profiles of the oscillating tone with those of the constant tone. There were no clear differences in the behaviors of the background magnetic field/density between the examples. In Figure S7, we show the hot electron distributions during the oscillating tone of Figure 3. The time resolutions of HOPE (1.4–14.7 keV) and MagEIS (31–108 keV) were 23 s and 11 s, respectively, which did not allow the expected modulation sign to be found at a time scale of 1–2 s. Hence, the available observations here did not provide any evidence for local modulation. However, because the satellites were located in the midlatitude region, some undiscovered modulation processes near the source region (magnetic equator) cannot be excluded.

4.3. Artificial Trigger

In the past, artificial transmitters have been found to be able to trigger some oscillating tones [Bell *et al.*, 1983; Mielke *et al.*, 1992]. In Figure S8, we present the satellite footprints of the events of Figures 2–5. The latitudes of the satellite footprints of different events did not show much difference, but their longitudes were widely separated. As shown in a list (https://en.wikipedia.org/wiki/List_of_VLF-transmitters), the VLF

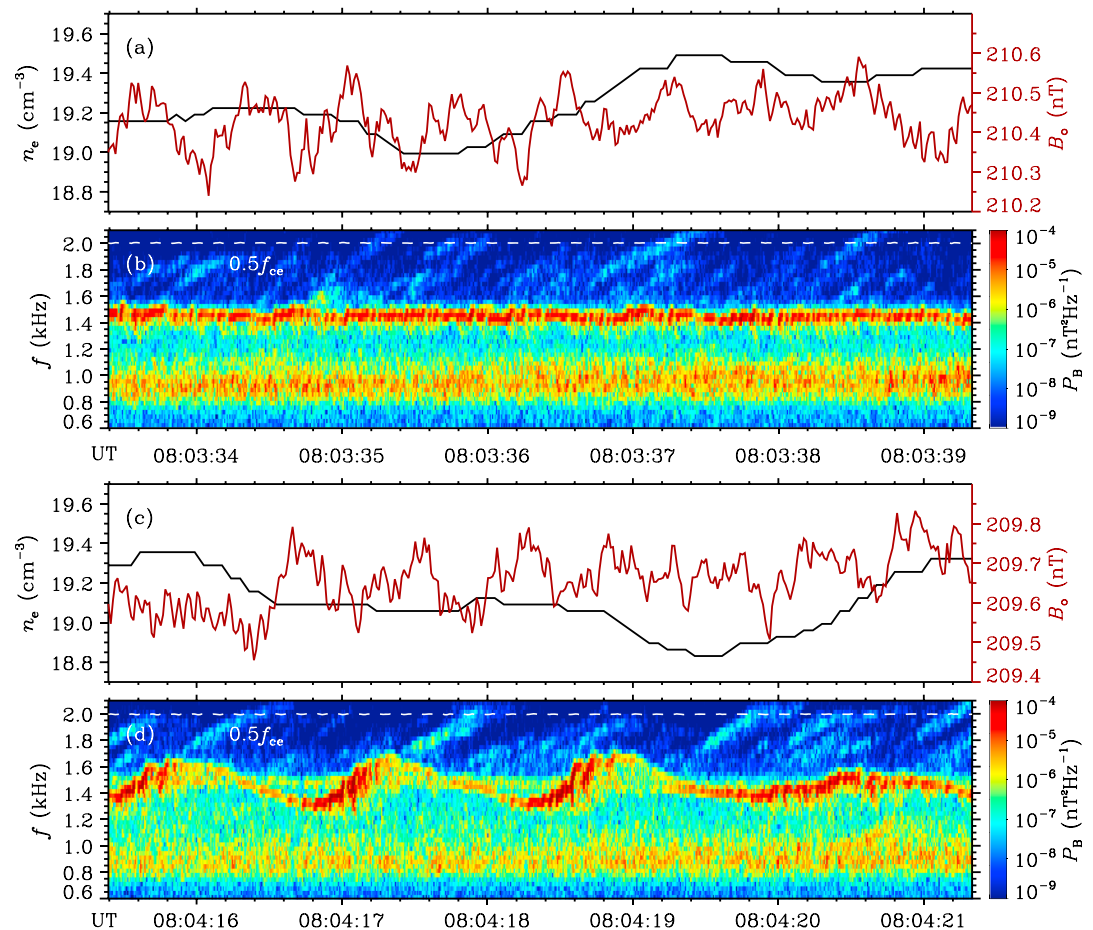


Figure 8. A comparison of the background conditions (magnetic field B_0 and electron density n_e) of the (a, b) constant and (c, d) oscillating tones.

transmitter stations were far away from those satellite footprints and their working frequencies (>10 kHz or <0.1 kHz) deviated significantly from the observed chorus frequency (1–4 kHz). Hence, the long-lived oscillating tone was unlikely to be associated with some artificial triggers but more likely to be a naturally occurring phenomenon.

5. Conclusions

Whistler-mode chorus emissions play an important role in radiation belt electron dynamics. In the frequency-time spectrogram, chorus emissions often appear as a hiss-like band and/or a series of short-lived (0.1–1 s) discrete elements. Here we presented some rarely reported chorus emissions with long-lived (up to 25 s) oscillating tones observed by the Van Allen Probes in the dayside (MLT ~ 9 –14) midlatitude ($|\text{MLAT}| > 15^\circ$) region during some weak or moderate substorms. The oscillating tones are found to behave either regularly or irregularly. Regarding the regularly oscillating tones, their frequency sweep range was up to ~ 1 kHz (Figure 4), with a repetition period of ~ 1 –2 s. Under certain circumstances, the regularly oscillating tone could transform into a nearly constant tone (with a relatively narrow frequency sweep range). Over every period of the oscillating tones, the rising part had a larger intensity and frequency sweep rate than the falling part, analogous to the situation of short-lived oscillating tones [Hospodarsky *et al.*, 2016, Figure 10.3c]. In contrast, neither the wave intensity nor the frequency sweep rate exhibited significant differences between the rising parts and falling parts of the irregularly oscillating tones. All of the regularly oscillating tones that we found had quasi-parallel propagation, while the irregularly oscillating tones could propagate either quasi-parallel or highly oblique to the background magnetic field. We suggest that the oscillating tone chorus was a natural phenomenon rather than an artificially triggered incident.

These highly coherent oscillating tones might be nonlinearly triggered by the accompanying hiss-like bands [Hansen, 1963; Helliwell, 1967]. The triggering of a rising tone by the hiss-like band, the evolution of a rising tone into a constant tone, and the transformation between an oscillating tone and a constant tone have been observed. The rising parts of oscillating tones are found to exhibit spectral characteristics analogous to those of the accompanying discrete rising tones. In the framework of nonlinear cyclotron resonance [Omura *et al.*, 2008; Omura and Nunn, 2011; Nunn and Omura, 2012], risers are generated in the region downstream of the equator, while the upstream of the equator is the generation region of fallers. A quasi-periodic transfer between the two types of generation regions will produce such oscillating tone chorus [Smith and Nunn, 1998]. Note that the repetition period of the oscillating tones is comparable to the bounce period of tens of keV electrons at $L = 5-6$. However, as shown in previous nonlinear simulations [Omura *et al.*, 2008; Omura and Nunn, 2011; Nunn and Omura, 2012], the typical duration of chorus elements is about 0.1–1.0 s, 10–100 times smaller than that of the observed oscillating tone. The details of the generation and evolution of such a long-lived oscillating tone chorus need to be investigated both theoretically and experimentally in the future.

Some subpackets with much shorter durations (<0.07 s) were embedded in the oscillating/constant tones. For constant tones and the rising parts of oscillating tones, the subpackets exhibited a rising frequency feature, analogous to the situation shown by Santolik *et al.* [2014] for a discrete rising tone. For the falling parts of oscillating tones, the frequency sweep of subpackets was indistinct. If the subpackets embedded in the oscillating tones commonly possess the rising frequency characteristics, the wave generation region will always be located downstream of the equator [Smith and Nunn, 1998] and the scenario that the generation region transfer produces oscillating tones will be doubtful. In the future, the observations with higher resolutions in both frequency and time will be required to resolve this ambiguity.

Another possible reason for the wave frequency oscillation is modulation by some physical quantities. The cold electron density and the background magnetic field locally measured by satellites did not show any correlation with the chorus wave frequency. The time resolution of hot electron data was not sufficient to allow the correlation analysis between hot electron distributions and chorus wave frequencies. Hence, the local observations did not provide any evidence for the potential modulation effect. However, because the satellites were located in the midlatitude region, some undiscovered modulation processes near the source region (magnetic equator) cannot be excluded.

Acknowledgments

We acknowledge EMFISIS, EFW, and ECT teams for the use of data, acknowledge J.H. King, N. Papatashvili, and CDAWeb for providing interplanetary parameters and magnetospheric indices, and acknowledge C. Torrence and G. Compo for providing the wavelet analysis software. The Van Allen Probes data are available at the websites: EMFISIS, <http://emfisis.physics.uiowa.edu/Flight/>; EFW, <http://www.space.umn.edu/rbspew-data/>; and ECT, http://www.rbsp-ect.lanl.gov/data_pub/. The interplanetary parameters and geomagnetic indices are obtained at the CDAWeb (http://cdaweb.gsfc.nasa.gov/cdaweb/istp_public/). This work was supported by the National Natural Science Foundation of China grants 41631071, 41422405, 41274174, 41174125, 41131065, 41421063, 41231066, and 41304134; the Chinese Academy of Sciences grant KZCX2-EW-QN510 and KZZD-EW-01-4; the CAS Key Research Program of Frontier Sciences grant QYZDB-SSW-DQC015, the National Key Basic Research Special Foundation of China grant 2011CB811403; and the Fundamental Research Funds for the Central UniversitiesWK2080000077. LC acknowledges NSF grant 1405041 through the Geospace Environment Modeling program.

References

- Bell, T. F., U. S. Inan, I. Kimura, H. Matsumoto, T. Mukai, and K. Hashimoto (1983), EXOS-B/siple station VLF wave-particle interaction experiments: 2. Transmitter signals and associated emissions, *J. Geophys. Res.*, **88**(A1), 295–309, doi:10.1029/JA088iA01p00295.
- Blake, J. B., et al. (2013), The Magnetic Electron Ion Spectrometer (MagEIS) instruments aboard the Radiation Belt Storm Probes (RBS) spacecraft, *Space Sci. Rev.*, **179**, 383–421, doi:10.1007/s11214-013-9991-8.
- Brice, N. (1963), An explanation of triggered very-low-frequency emissions, *J. Geophys. Res.*, **68**, 4626, doi:10.1029/JZ068i015p04626.
- Burtis, W. J., and R. A. Helliwell (1976), Magnetospheric chorus—Occurrence patterns and normalized frequency, *Planet. Space Sci.*, **24**, 1007–1024, doi:10.1016/0032-0633(76)90119-7.
- Carpenter, D. L. (2014), *The Early History of Very Low Frequency (VLF) Radio Research at Stanford*, [Available at http://vlf.stanford.edu/research_ext/history-very-low-frequency-vlf-radio-research-stanford/].
- Cattell, C., A. Breneman, S. Thaller, J. Wygant, C. Kletzing, and W. Kurth (2015), Van Allen Probes observations of unusually low frequency whistler mode waves observed in association with moderate magnetic storms: Statistical study, *Geophys. Res. Lett.*, **42**, 7273–7281, doi:10.1002/2015GL065565.
- Colpitts, C. A., C. A. Cattell, M. Engebretson, M. Broughton, S. Tian, J. Wygant, A. Breneman, and S. Thaller (2016), Van Allen Probes observations of cross-scale coupling between electromagnetic ion cyclotron waves and higher-frequency wave modes, *Geophys. Res. Lett.*, **43**, 11,510–11,518, doi:10.1002/2016GL071566.
- Funsten, H. O., et al. (2013), Helium, Oxygen, Proton, and Electron (HOPE) mass spectrometer for the Radiation Belt Storm Probes mission, *Space Sci. Rev.*, **179**, 423–484, doi:10.1007/s11214-013-9968-7.
- Gao, Z., Z. Su, H. Zhu, F. Xiao, H. Zheng, Y. Wang, C. Shen, and S. Wang (2016), Intense low-frequency chorus waves observed by Van Allen Probes: Fine structures and potential effect on radiation belt electrons, *Geophys. Res. Lett.*, **43**, 967–977, doi:10.1002/2016GL067687.
- Hansen, S. F. (1963), A mechanism for the production of certain types of very-low-frequency emissions, *J. Geophys. Res.*, **68**(21), 5925–5935, doi:10.1029/JZ068i021p05925.
- Helliwell, R. A. (1967), A theory of discrete VLF emissions from the magnetosphere, *J. Geophys. Res.*, **72**, 4773–4790, doi:10.1029/JZ072i019p04773.
- Horne, R. B., and R. M. Thorne (1998), Potential waves for relativistic electron scattering and stochastic acceleration during magnetic storms, *Geophys. Res. Lett.*, **25**, 3011–3014, doi:10.1029/98GL01002.
- Horne, R. B., et al. (2005), Wave acceleration of electrons in the Van Allen radiation belts, *Nature*, **437**, 227–230, doi:10.1038/nature03939.
- Hospodarsky, G. B., W. S. Kurth, C. A. Kletzing, S. R. Bounds, O. Santolik, R. M. Thorne, W. Li, T. F. Averkamp, J. R. Wygant, and J. W. Bonnell (2016), Plasma wave measurements from the Van Allen Probes, in *Magnetosphere-Ionosphere Coupling in the Solar System*, edited by C. R. Chappell *et al.*, pp. 127–143, John Wiley, Hoboken, N. J., doi:10.1002/9781119066880.ch10.
- Katoh, Y., and Y. Omura (2013), Effect of the background magnetic field inhomogeneity on generation processes of whistler-mode chorus and broadband hiss-like emissions, *J. Geophys. Res. Space Physics*, **118**, 4189–4198, doi:10.1002/jgra.50395.
- Kennel, C. F. (1969), Consequences of a magnetospheric plasma, *Rev. Geophys.*, **7**, 379–419, doi:10.1029/RG007i001p00379.

- Kennel, C. F., and H. E. Petschek (1966), Limit on stably trapped particle fluxes, *J. Geophys. Res.*, *71*, 1–28, doi:10.1029/JZ071i001p00001.
- King, J. H., and N. E. Papitashvili (2005), Solar wind spatial scales in and comparisons of hourly Wind and ACE plasma and magnetic field data, *J. Geophys. Res.*, *110*, A02104, doi:10.1029/2004JA010649.
- Kletzing, C. A., et al. (2013), The Electric and Magnetic Field Instrument Suite and Integrated Science (EMFISIS) on RBSP, *Space Sci. Rev.*, *179*, 127–181, doi:10.1007/s11214-013-9993-6.
- Li, W., R. M. Thorne, V. Angelopoulos, J. W. Bonnell, J. P. McFadden, C. W. Carlson, O. LeContel, A. Roux, K. H. Glassmeier, and H. U. Auster (2009), Evaluation of whistler-mode chorus intensification on the nightside during an injection event observed on the THEMIS spacecraft, *J. Geophys. Res.*, *114*, A00C14, doi:10.1029/2008JA013554.
- Li, W., R. M. Thorne, J. Bortnik, Y. Nishimura, and V. Angelopoulos (2011a), Modulation of whistler mode chorus waves: 1. Role of compressional Pc4-5 pulsations, *J. Geophys. Res.*, *116*, A06205, doi:10.1029/2010JA016312.
- Li, W., J. Bortnik, R. M. Thorne, Y. Nishimura, V. Angelopoulos, and L. Chen (2011b), Modulation of whistler mode chorus waves: 2. Role of density variations, *J. Geophys. Res.*, *116*, A06206, doi:10.1029/2010JA016313.
- Li, W., R. M. Thorne, J. Bortnik, X. Tao, and V. Angelopoulos (2012), Characteristics of hiss-like and discrete whistler-mode emissions, *Geophys. Res. Lett.*, *39*, L18106, doi:10.1029/2012GL053206.
- Mauk, B. H., N. J. Fox, S. G. Kanekal, R. L. Kessel, D. G. Sibeck, and A. Ukhorskiy (2013), Science objectives and rationale for the Radiation Belt Storm Probes mission, *Space Sci. Rev.*, *179*, 3–27, doi:10.1007/s11214-012-9908-y.
- Meredith, N. P., R. B. Horne, and R. R. Anderson (2001), Substorm dependence of chorus amplitudes: Implications for the acceleration of electrons to relativistic energies, *J. Geophys. Res.*, *106*, 13,165–13,178, doi:10.1029/2000JA900156.
- Mielke, T. A., C. J. Elkins, R. A. Helliwell, and U. S. Inan (1992), Excitation of whistler mode signals via injection of polarized VLF waves with the simple transmitter, *Radio Sci.*, *27*(1), 31–46, doi:10.1029/91RS02457.
- Nunn, D. (1990), The numerical simulation of VLF nonlinear wave-particle interactions in collision-free plasmas using the Vlasov hybrid simulation technique, *Comput. Phys. Commun.*, *60*, 1–25, doi:10.1016/0010-4655(90)90074-B.
- Nunn, D., and Y. Omura (2012), A computational and theoretical analysis of falling frequency VLF emissions, *J. Geophys. Res.*, *117*, A08228, doi:10.1029/2012JA017557.
- Nunn, D., M. Rycroft, and V. Trakhtengerts (2005), A parametric study of the numerical simulations of triggered VLF emissions, *Ann. Geophys.*, *23*, 3655–3666, doi:10.5194/angeo-23-3655-2005.
- Omura, Y., and D. Nunn (2011), Triggering process of whistler mode chorus emissions in the magnetosphere, *J. Geophys. Res.*, *116*, A05205, doi:10.1029/2010JA016280.
- Omura, Y., Y. Katoh, and D. Summers (2008), Theory and simulation of the generation of whistler-mode chorus, *J. Geophys. Res.*, *113*, A04223, doi:10.1029/2007JA012622.
- Pickett, J., et al. (2005), Multi-point CLUSTER observations of VLF risers, fallers and hooks at and near the plasmopause, in *Multiscale Processes in the Earth's Magnetosphere: From Interball to Cluster*, pp. 307–328, Springer, Dordrecht, Netherlands.
- Reeves, G. D., et al. (2013), Electron acceleration in the heart of the Van Allen radiation belts, *Science*, *341*(6149), 991–994, doi:10.1126/science.1237743.
- Santolík, O., D. A. Gurnett, J. S. Pickett, M. Parrot, and N. Cornilleau-Wehrin (2003a), Spatio-temporal structure of storm-time chorus, *J. Geophys. Res.*, *108*(A7), 1278, doi:10.1029/2002JA009791.
- Santolík, O., M. Parrot, and F. Lefeuvre (2003b), Singular value decomposition methods for wave propagation analysis, *Radio Sci.*, *38*(1), 1010, doi:10.1029/2000RS002523.
- Santolík, O., D. A. Gurnett, J. S. Pickett, M. Parrot, and N. Cornilleau-Wehrin (2004), A microscopic and nanoscopic view of storm-time chorus on 31 March 2001, *Geophys. Res. Lett.*, *31*, L02801, doi:10.1029/2003GL018757.
- Santolík, O., D. A. Gurnett, J. S. Pickett, J. Chum, and N. Cornilleau-Wehrin (2009), Oblique propagation of whistler mode waves in the chorus source region, *J. Geophys. Res.*, *114*, A00F03, doi:10.1029/2009JA014586.
- Santolík, O., C. Kletzing, W. Kurth, G. Hospodarsky, and S. Bounds (2014), Fine structure of large-amplitude chorus wave packets, *Geophys. Res. Lett.*, *41*, 293–299, doi:10.1002/2013GL058889.
- Smith, A. J., and D. Nunn (1998), Numerical simulation of VLF risers, fallers, and hooks observed in Antarctica, *J. Geophys. Res.*, *103*(A4), 6771–6784, doi:10.1029/97JA03396.
- Spence, H. E., et al. (2013), Science goals and overview of the Energetic Particle, Composition, and Thermal Plasma (ECT) suite on NASA's Radiation Belt Storm Probes (RBSP) mission, *Space Sci. Rev.*, *179*, 311–336, doi:10.1007/s11214-013-0007-5.
- Su, Z., et al. (2014a), Nonstorm time dynamics of electron radiation belts observed by the Van Allen Probes, *Geophys. Res. Lett.*, *41*, 229–235, doi:10.1002/2013GL058912.
- Su, Z., et al. (2014b), Quantifying the relative contributions of substorm injections and chorus waves to the rapid outward extension of electron radiation belt, *J. Geophys. Res. Space Physics*, *119*, 10,023–10,040, doi:10.1002/2014JA020709.
- Su, Z., et al. (2014c), Intense duskside lower band chorus waves observed by Van Allen Probes: Generation and potential acceleration effect on radiation belt electrons, *J. Geophys. Res. Space Physics*, *119*, 4266–4273, doi:10.1002/2014JA019919.
- Summers, D., R. M. Thorne, and F. Xiao (1998), Relativistic theory of wave-particle resonant diffusion with application to electron acceleration in the magnetosphere, *J. Geophys. Res.*, *103*, 20,487–20,500, doi:10.1029/98JA01740.
- Summers, D., C. Ma, N. P. Meredith, R. B. Horne, R. M. Thorne, D. Heynderickx, and R. R. Anderson (2002), Model of the energization of outer-zone electrons by whistler-mode chorus during the October 9, 1990 geomagnetic storm, *Geophys. Res. Lett.*, *29*(24), 2174, doi:10.1029/2002GL016039.
- Thorne, R. M., and C. F. Kennel (1967), Quasi-trapped VLF propagation in the outer magnetosphere, *J. Geophys. Res.*, *72*, 857–870, doi:10.1029/JZ072i003p00857.
- Thorne, R. M., et al. (2013), Rapid local acceleration of relativistic radiation-belt electrons by magnetospheric chorus, *Nature*, *504*, 411–414, doi:10.1038/nature12889.
- Tsurutani, B. T., and E. J. Smith (1974), Postmidnight chorus: A substorm phenomenon, *J. Geophys. Res.*, *79*(1), 118–127, doi:10.1029/JA079i001p00118.
- Tsyganenko, N. A., and M. I. Sitnov (2005), Modeling the dynamics of the inner magnetosphere during strong geomagnetic storms, *J. Geophys. Res.*, *110*, A03208, doi:10.1029/2004JA010798.
- Van Compernelle, B., X. An, J. Bortnik, R. M. Thorne, P. Pribyl, and W. Gekelman (2015), Excitation of chirping whistler waves in a laboratory plasma, *Phys. Rev. Lett.*, *114*, 245002, doi:10.1103/PhysRevLett.114.245002.
- Wygant, J., et al. (2013), The electric field and waves instruments on the Radiation Belt Storm Probes mission, *Space Sci. Rev.*, *179*(1–4), 183–220, doi:10.1007/s11214-013-0013-7.